J. Fluid Mech. (1970), *vol.* 42, *part* 4, *pp.* 657–670
Printed in Great Britain

On the generation of Kelvin-type waves by atmospheric disturbances

By RICHARD E. THOMSON
Institute of Oceanography, University of British Columbia, Canada

(Received 24 June 1969)

This paper considers the surface response of a semi-infinite, uniformly rotating, constant depth, homogeneous ocean to a variable atmospheric force. For a general wind and pressure system it is shown that forced Kelvin-type waves can be generated and that only the longshore wind component and the pressure can generate them. In particular a semi-infinite wind and moving pressure pattern are shown to generate Kelvin waves that travel away from the force discontinuities at the speed of shallow-water waves. The waves in the latter case exhibit a frequency shift typical of non-dispersive waves from a moving source. Some numerical values for the amplitudes of the Kelvin waves are also given.

1. Introduction

The generation of long waves by initially applied forces on the surface of a uniformly rotating infinite ocean has been theoretically investigated by such authors as Crease (1956) and Mysak (1969). Similar investigations for a non-uniformly rotating ocean have been carried out by Veronis & Stommel (1956) and by Longuet-Higgins (1965) using the β-plane approximation. For the case of a semi-infinite ocean Kajiura (1962) considered the possibility of Kelvin-type waves being generated at the boundary. Using a Green's function approach he investigated the surface response to an atmospheric disturbance of rectangular-horizontal extent and was able to show that the solution for large distances from the source but close to the wall did behave as a Kelvin wave.

In this paper we also consider the response of the sea surface to atmospheric forces in the presence of an infinite boundary, but instead of a Green's function approach we solve the initial boundary-value problem using transform methods. The result is that the response behaves as a forced Kelvin wave and that this wave appears as part of the exact solution. Also, we find that only the longshore component of the wind-stress and pressure gradient can generate these waves, in agreement with Kajiura.

In § 2 a partial differential equation for the forced surface elevation is derived from the linearized shallow-water equations. Transform methods are then used in § 3 to determine the sea surface response to a general space-time wind-stress and pressure in the presence of an infinite boundary. Section 4 is devoted to a discussion of that part of the solution which gives rise to Kelvin-type waves. These results are used in §§ 5 and 6 for specific examples: (i) a non-travelling divergent longshore wind pattern, and (ii) a moving pressure source, respectively. Through the application of a Tauberian theorem, the steady-state response for large times is shown in §7 to be zero in each case. In §8 a physical discussion of the results found in §§4 and 5 is given. Finally, in §9 some numerical values for the amplitudes and velocities are presented.

2. Equations of motion

We consider a homogeneous, uniformly rotating ocean in which non-linearities and bottom friction are neglected. Further, we assume that the waves are sufficiently long for the hydrostatic equation to be valid. Then the vertically integrated equations of momentum and mass conservation are:

$$\left.\begin{aligned}\frac{\partial u}{\partial t}-fv &= -g\frac{\partial \zeta}{\partial x}-\frac{1}{\rho}\frac{\partial P_a}{\partial x}+\frac{\tau^x}{\rho h},\\ \frac{\partial v}{\partial t}+fu &= -g\frac{\partial \zeta}{\partial y}-\frac{1}{\rho}\frac{\partial P_a}{\partial y}+\frac{\tau^y}{\rho h},\end{aligned}\right\} \tag{2.1}$$

$$\frac{\partial(hu)}{\partial x}+\frac{\partial(hv)}{\partial y} = -\frac{\partial \zeta}{\partial t}, \tag{2.2}$$

in which the hydrostatic equation $P = P_a+\rho g(\zeta-z)$ has been used, and where x, y are horizontal Cartesian co-ordinates, z is measured vertically upwards, t is the time, ζ is the sea-surface elevation, u, v are the velocity components along x, y, and h is the mean depth, assumed constant. g is the acceleration of gravity, f the Coriolis parameter, ρ the water density, P_a the air pressure on the sea surface and τ^x, τ^y are the components of the wind-stress in the x, y directions. Then from (2.1) we obtain

$$Nu = -\left(\frac{\partial^2}{\partial x\,\partial t}+f\frac{\partial}{\partial y}\right)\left(g\zeta+\frac{P_a}{\rho}\right)+\frac{1}{\rho h}\left(\frac{\partial \tau^x}{\partial t}+f\tau^y\right), \tag{2.3}$$

$$Nv = \left(-\frac{\partial^2}{\partial y\,\partial t}+f\frac{\partial}{\partial x}\right)\left(g\zeta+\frac{P_a}{\rho}\right)+\frac{1}{\rho h}\left(\frac{\partial \tau^y}{\partial t}-f\tau^x\right), \tag{2.4}$$

where $N = f^2+\partial^2/\partial t^2$. Using equations (2.3) and (2.4) in (2.2) we obtain

$$\left(\nabla_2^2-\frac{N}{gh}\right)\frac{\partial \zeta}{\partial t} = F, \tag{2.5}$$

where
$$\left.\begin{aligned}F &= a\left[(\nabla\times\boldsymbol{\tau})^z+\frac{1}{f}\nabla_2\cdot\frac{\partial \boldsymbol{\tau}}{\partial t}-\frac{h}{f}\nabla_2^2\frac{\partial P_a}{\partial t}\right], \quad a = \frac{f}{\rho g h},\\ \boldsymbol{\tau} &= (\tau^x, \tau^y, 0) \quad \text{and} \quad \nabla_2^2 = \partial^2/\partial x^2+\partial^2/\partial y^2.\end{aligned}\right\} \tag{2.6}$$

In the general analysis of §§3 and 4 we will only require that $\boldsymbol{\tau}$ and P_a be bounded and in particular that they both are zero at $|y| = \infty$.

Our model consists of a semi-infinite ocean of constant depth h, bounded at $x = 0$ by a vertical wall. In this paper the analysis is carried through for an ocean in the half-plane $x > 0$; for an ocean in the half-plane $x < 0$ it is simply a matter of substituting $x = -x$ whenever it appears. Also we have assumed $f > 0$ so that the analysis is for the northern hemisphere; in the southern hemisphere we take $f < 0$. At the wall we require that the normal velocity component (u) vanish.

3. Response to a general wind and pressure field

We assume that at $t = 0$ a pressure (P_a) and a horizontal wind-stress distribution begin to quickly build up over the surface, which is initially at rest; i.e. $\zeta \equiv 0$ for $t < 0$.

We now define the Fourier–Laplace transform of $\Phi(x, y, t)$ by

$$\bar{\Phi}(x, \lambda, s) = \int_0^\infty \exp(-st)\,dt \int_{-\infty}^\infty \exp(i\lambda y)\,\Phi(x, y, t)\,dy \tag{3.1}$$

and specify the following conditions:

$$\left.\begin{aligned} \partial\zeta/\partial t = \zeta = 0 \quad &\text{at} \quad t \leqslant 0, \\ < M_1 \quad &\text{as} \quad t \to +\infty; \\ \partial\zeta/\partial y, \quad \zeta < M_2 \quad &\text{as} \quad |y| \to +\infty; \\ P_a, \quad \partial P_a/\partial y, \quad |\boldsymbol{\tau}| \to 0 \quad &\text{as} \quad t,\ |y| \to +\infty; \\ \partial\zeta/\partial x, \quad \zeta < M_3 \quad &\text{as} \quad x \to +\infty; \end{aligned}\right\} \tag{3.2a–d}$$

where the M_i are finite.

These conditions will be used to obtain the general transform of ζ as a function of P_a and $\boldsymbol{\tau}$.

Since (2.5) is a third-order differential equation in time, the Laplace transform method requires a knowledge of $\partial^2\zeta/\partial t^2$ at $t = 0$. In this paper such initial accelerations will be zero since atmospheric disturbances will be assumed continuous in time. Physically this is the most realistic situation, although mathematically there is no difficulty in allowing initial discontinuities for specific cases since they simply require the inclusion of the initial acceleration and forces.

With the above condition, and (3.2a,b,c) equation (2.5) transforms to

$$(d^2/dx^2 - k^2)\bar{\zeta}(x, \lambda, s) = s^{-1}\bar{F}^*(x, \lambda, s), \tag{3.3}$$

in which $k = (\lambda^2 + [f^2 + s^2]/c^2)^{\frac{1}{2}} > 0$ for λ real, $c^2 = gh$ and

$$\bar{F}^*(x, \lambda, s) = a[d(\overline{\tau^y}(x, \lambda, s) + sf^{-1}\overline{\tau^x}(x, \lambda, s))/dx + i\lambda(\overline{\tau^x}(x, \lambda, s) - sf^{-1}\overline{\tau^y}(x, \lambda, s)) - hf^{-1}(d^2/dx^2 - \lambda^2)s\overline{P_a}(x, \lambda, s)]. \tag{3.4}$$

The most general solution to (3.3) under condition (3.2d) is then

$$\bar{\zeta}(x, \lambda, s) = c(\lambda, s)\exp(-kx) - \frac{1}{2ks}\int_0^\infty G_k(x|x')\,\bar{F}^*(x', \lambda, s)\,dx', \tag{3.5}$$

where $G_k(x|x') = G(x|x'|k)$ is the Green's function

$$G_k(x|x') = \exp[-k|x - x'|]. \tag{3.6}$$

To determine $c(\lambda, s)$ we use the boundary condition $u = 0$ at $x = 0$. Taking the transform of (2.3), using conditions (3.2a,b,c) and substituting from (3.5) and (3.6) we obtain,

$$(i\lambda f+ks)\,c(\lambda,s) = \frac{i\lambda f-ks}{2ks}\int_0^\infty \exp(-kx')\,\overline{F}{}^*(x',\lambda,s)\,dx' + ah\left[\left(\frac{s}{f}\frac{\partial}{\partial x}-i\lambda\right)\overline{P_a}(0,\lambda,s)\right]-a\left[\frac{s}{f}\overline{\tau^x}(0,\lambda,s)+\overline{\tau^y}(0,\lambda,s)\right], \quad (3.7)$$

whereby (3.5) becomes, after some manipulation,

$$\frac{2ksf}{a}\bar{\zeta}(x,\lambda,s) = \frac{i\lambda f-ks}{i\lambda f+ks}\left[T_1(x,\lambda,s)-h\frac{f^2+s^2}{c^2}P_1(x,\lambda,s)\right]+i\lambda T_2(x,\lambda,s) + kT_3(x,\lambda,s)+h\frac{f^2+s^2}{c^2}P_2(x,\lambda,s)-2khs\overline{P_a}(x,\lambda,s), \quad (3.8)$$

in which

$$T_1(x,\lambda,s) = \int_0^\infty \exp[-k(x+x')][(fk-i\lambda s)\overline{\tau^y}(x',\lambda,s)+(i\lambda f+ks)\overline{\tau^x}(x',\lambda,s)]\,dx',$$

$$T_2(x,\lambda,s) = \int_0^\infty G_k(x|x')[s\overline{\tau^y}(x',\lambda,s)-f\overline{\tau^x}(x',\lambda,s)]\,dx',$$

$$T_3(x,\lambda,s) = \int_0^\infty \operatorname{sgn}(x-x')\exp[-k|x-x'|][f\overline{\tau^y}(x',\lambda,s)+s\overline{\tau^x}(x',\lambda,s)]\,dx',$$

$$P_1(x,\lambda,s) = s\int_0^\infty \exp[-k(x+x')]\,\overline{P_a}(x',\lambda,s)\,dx',$$

$$P_2(x,\lambda,s) = s\int_0^\infty G_k(x|x')\,\overline{P_a}(x',\lambda,s)\,dx', \quad (3.9)$$

and

$$\operatorname{sgn}(q) = +1 \quad (q>0)$$
$$= -1 \quad (q<0).$$

The surface response is then found by taking the inverse, viz.

$$\zeta(x,y,t) = \frac{1}{4\pi^2 i}\int_{-\infty}^{\infty}\exp(-i\lambda y)\,d\lambda\int_{\gamma+i\infty}^{\gamma-i\infty}\exp(st)\bar{\zeta}(x,\lambda,s)\,ds. \quad (3.10)$$

In the s plane γ is chosen so that any singularities lie to the left of the inversion path (see figure 1), while in the λ plane the inversion path must be suitably indented above or below any singularities on the real λ axis; the appropriate indentations being determined by the Sommerfeld radiation condition.

4. Kelvin-wave solutions

As seen from expression (3.8), only the first two terms can possibly contribute poles in the s and λ planes, other than at $s = 0$, which are not totally attributable to the force. Since we are inverting our transform with respect to s first, these poles are at $s = -i\lambda c$ and $s = -if|\lambda|/\lambda$ (since $k > 0$) as derived from $i\lambda f+ks = 0$, and thus arise entirely from the wall boundary condition. Similarly, when we first evaluate for s-plane poles which arise from the explicit form of the force we will obtain poles in the λ plane for the zeros of $i\lambda f + k_{sj}s_j$; where $k_{sj}s_j$ is evaluated at the s-plane poles, s_j, of the force. It is these terms which give rise to Kelvin waves.

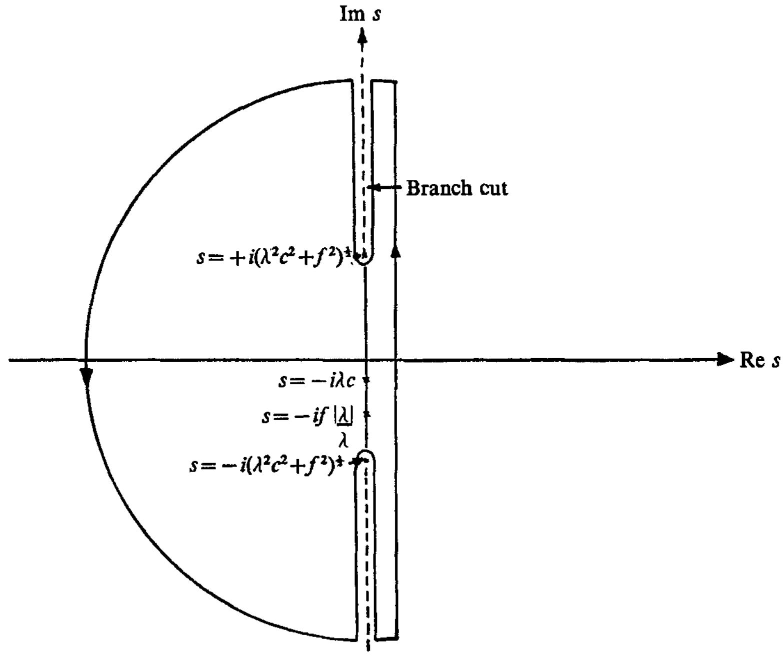

FIGURE 1. Path of integration in the s plane, $s = \mathrm{Re}\, s + i\,\mathrm{Im}\, s$. (----, branch cuts; $\times$, singularities). Singularities due to the transform of a particular force are not shown.

To partly demonstrate the above remarks, without specifying a force, we consider the poles at the zeros of $i\lambda f + ks$ in the s plane. Let $\zeta_1(x,y,t)$ represent their contribution to the surface response. Now because the force is assumed bounded for all t, the poles and/or branch points it contributes in the s plane will also lie on or to the left of the imaginary s axis. Thus in this plane we close the inversion contour, Γ, to the right for $t < 0$ and to the left for $t > 0$. Hence $\zeta_1 = 0$ for $t < 0$. For $t > 0$ the contribution from the pole at $s = -i\lambda c$ for the first two terms of (3.8) is, using (3.10) and Cauchy's residue theorem,

$$\zeta_1(x,y,t) = \int_0^\infty dx' \exp\left[-\frac{f}{c}(x+x')\right]\int_{-\infty}^{\infty} d\lambda \exp[-i\lambda(y+ct)][a_1\overline{\overline{\tau^y}}(x',\lambda,s) - a_2\lambda\overline{\overline{P_a}}(x',\lambda,s)]_{s=-i\lambda c}. \tag{4.1}$$

in which $$a_1 = -a/2\pi \quad \text{and} \quad a_2 = +iha/2\pi, \tag{4.2}$$

while that from the pole at $s = -if|\lambda|/\lambda$, is zero. It is easily seen that (4.1) represents a Kelvin wave in which the wave-number λ will be determined by the explicit form of the force.

5. Response to a non-travelling wind pattern

In order to demonstrate the remarks of §4 we take as an example a disturbance that is stationary in space but transient in time. One such form satisying boundary condition (3.2c) is

$$\left.\begin{aligned} \tau^y &= \tau_0 H(t)\sin\omega t \exp(-\sigma t) H(y)\exp(-\mu y), \\ \tau^x &= P_a = 0, \end{aligned}\right\} \tag{5.1}$$

where τ_0 = constant, μ and σ are real (>0), ω is real and $H(q)$ is the unit step function. This forcing field could be regarded as a crude approximation to that caused by successive, large onshore moving weather systems in which the pressure difference between each storm's centre and edge is small. Then, applying (3.1) we find

$$\overline{\tau^y} = -\tau_0 \frac{\omega}{(s+\sigma)^2+\omega^2} \frac{1}{i\lambda-\mu}. \tag{5.2}$$

Substituting this into (4.1) we obtain poles at $\lambda_0 = -i\mu$ and $\lambda_{\pm} = (\pm\omega - i\sigma)/c$.

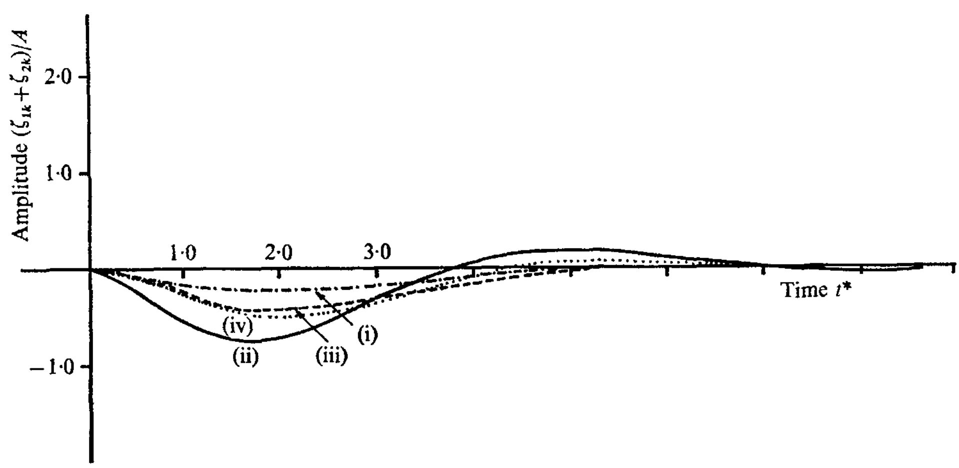

Figure 2. Plots of the amplitudes of the wind-generated Kelvin waves [(5.3)+(5.5)] at fixed longshore position, $y = y_0 < 0$, for increasing time $t^* = \omega(t+y_0/c)$, for four given values of the decay frequency, $\sigma-\mu c$ ($\omega \neq 0$). (i) $\sigma = \mu c = \omega$; (ii) $\sigma = \frac{1}{2}\omega$, $\mu c = 2\omega$; (iii) $\sigma = \frac{1}{2}\omega$, $\mu c = \omega$; (iv) $\sigma = 2\omega$, $\mu c = \frac{1}{2}\omega$.

Evaluation is then a straightforward application of Cauchy's residue theorem provided we conform to the following condition: the contour is closed above for $y+ct < 0$ and below for $y+ct > 0$. This ensures that integration along the large semi-circle of the inversion path vanishes in each case, or, which amounts to the same thing, that any solution be bounded. In the analysis to follow $\sigma > 0$ to avoid having poles on the imaginary s axis, which, depending on whether $f \gtrless \omega$, could necessitate an inversion contour other than that in figure 1. Equation (4.1) then becomes

$$\zeta_{1\nu}(x,y,t) = A\{\{\cos[\kappa(y+ct)] + \alpha\sin[\kappa(y+ct)]\}\exp[-m(y+ct)] - \exp[-\mu(y+ct)]\}H(y+ct), \tag{5.3}$$

where $(\kappa, m) = c^{-1}(\omega, \sigma)$ are horizontal wave-numbers, $\alpha = (\sigma - \mu c)/\omega$ and

$$A = (\tau_0/\rho c)\,\omega/[\omega^2 + (\sigma - \mu c)^2]\exp(-fx/c). \tag{5.4}$$

Following §4 we next evaluate the first term of (3.8) at the poles in the s plane due to the explicit form of the force, i.e. at $s_{\pm} = \pm i\omega - \sigma$ from (5.2). Further inversion in the λ plane for the poles at the zeros of $i\lambda f + k_{s_{\pm}} s_{\pm}$ gives a contribution $\zeta_{2\nu}$ such that

$$\zeta_{2\nu}(x,y,t) = -\zeta_{1\nu}(x,y,t)\frac{H(y)}{H(y+ct)} - A\exp[-\mu(y+ct)]\,H(y+ct). \tag{5.5}$$

It is easily seen that the combination of (5.3) and (5.5) represents a wind-forced Kelvin wave plus a surge-like term moving away from the forcing region ($y > 0$) with the long wave speed, c; (see figure 2).

Although it is not the purpose of this paper to investigate all the possible long waves generated by a particular disturbance, we will briefly outline their general behaviour. If we include all terms of (3.8) we find the following: (i) no contribution for the poles at $s = 0$; (ii) for the poles at $s = s_{\pm}$ all terms, excluding the first (which gave (5.5)), give a response ζ_w, which, using the method of steepest descent, can be shown to behave as

$$\lim_{\substack{\mu,\sigma\to 0^+ \\ (f-\omega)^{\frac{1}{2}}r/c\to\infty}} \zeta_w(x,y,t) \sim A \lim_{\sigma\to 0^+}[\exp(-\sigma t)]\sin(\omega t)\left\{\frac{\exp[-(f^2-\omega^2)^{\frac{1}{2}}r/c]}{(f^2-\omega^2)^{\frac{1}{4}}(r/c)^{\frac{1}{2}}}\frac{1}{\cos\theta} - (2\pi)^{\frac{1}{2}}\exp[-(f^2-\omega^2)^{\frac{1}{2}}y/c]\right\}H(y), \tag{5.6}$$

where $A = \dfrac{1}{(8\pi)^{\frac{1}{2}}}\dfrac{\tau_0}{\rho c}\dfrac{1}{(f^2-\omega^2)^{\frac{1}{4}}}$, $\quad (x,y) = r(\cos\theta, \sin\theta)\quad$ and $\quad |\theta| < \frac{1}{2}\pi$;

(iii) for the poles at $s_{\pm}$ the first term has, besides the Kelvin-wave poles, a pole at $\lambda = -i\mu$ where for σ, $\mu \to 0^+$ the resulting displacement ζ_μ behaves as

$$\lim_{\mu,\sigma\to 0^+}\zeta_\mu(x,y,t) = -\frac{\tau_0}{\rho c}\frac{f}{\omega}\frac{1}{(f^2-\omega^2)^{\frac{1}{2}}}\lim_{\sigma\to 0^+}[\exp(-\sigma t)]\cos(\omega t)\exp[-(f^2-\omega^2)^{\frac{1}{2}}x/c]\,H(y), \tag{5.7}$$

and finally (iv) the branch cut integration for $s = \pm i(\lambda^2c^2 + f^2)^{\frac{1}{2}}$ (when $k = 0$) gives the following double integral, ζ_{bc}, at $x = 0$;

$$\zeta_{bc}(0,y,t) = E\int\int_{-\infty}^{+\infty}\frac{\exp(-i\lambda y)}{q^2-\lambda^2c^2}\frac{(\omega^2+\sigma^2-q^2)\sin(qt) - 2\sigma q\cos(qt)}{(\omega^2+\sigma^2-q^2)^2 + 4q^2\sigma^2}\frac{q}{(q^2-\beta^2)^{\frac{1}{2}}}\,dq\,d\lambda \tag{5.8}$$

where $\qquad E = \tau_0 if\omega c/\pi^2 \quad$ and $\quad \beta^2 = \lambda^2c^2 + f^2$.

For $\sigma \to 0^+$ it is straightforward to show that (5.8) consists of standing type waves of the form, $\sin(\omega t)\sin(\omega y/c)$, $\cos(\omega y/c)\sin(\omega t)$, ... while the use of Laplace's method [see Carrier, Krook & Pearson (1966, p. 256) for a description of this method] for the branch points of (5.8) yields terms like

$$\lim_{t\to+\infty}\zeta_{bc}(0,y,t) \sim \frac{\exp(-\sigma t)}{t^{\frac{1}{2}}}\cos(\omega t)\exp[-(f^2-\omega^2)^{\frac{1}{2}}y/c] + O(t^{-\frac{3}{2}}). \tag{5.9}$$

6. Response to a moving storm

As a final example we determine the Kelvin-wave response to a moving pressure source, which for simplicity will be represented by a delta function. Later in this section we will give some justification for such a pressure distribution.

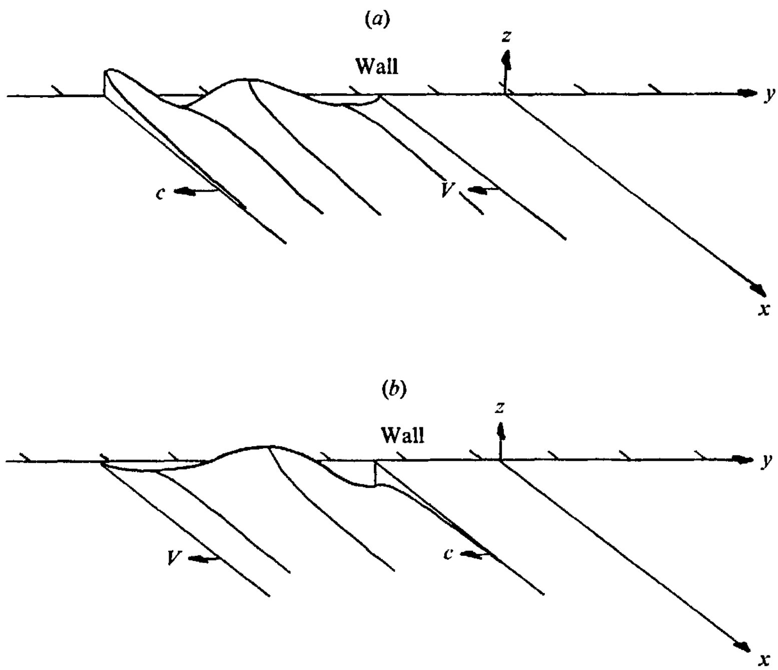

FIGURE 3. Schematic diagram of the regions occupied by the pressure-generated Kelvin waves of §6 for a storm moving in the negative y direction: (a) $c > V$; (b) $c < V$.

We consider the form

$$\left.\begin{aligned} &\tau^x = \tau^y = 0, \\ &P_a = P\gamma^2\delta(y+Vt)\delta(x-x_0)\sin(\omega t)\exp(-\sigma t) \quad (t \geqslant 0,\ x_0 > 0), \end{aligned}\right\} \tag{6.1}$$

where P_a is now the pressure difference, at sea level, between the centre of the storm and the undisturbed pressure far from the disturbance, and in which $P =$ constant, V is the speed of the storm, x_0 is the distance from the coast, ω, σ (>0) are real and γ is a measure of the storm's width [we again retain $\sigma > 0$ so that the inversion contour in the s plane has the form of figure 1]. Then using (3.1) we find

$$\overline{P}_a = P\gamma^2\delta(x-x_0)\frac{\omega}{(s+\sigma+i\lambda V)^2+\omega^2}, \tag{6.2}$$

which substituted into (4.1) yields poles at $\lambda_\pm = (\pm\omega+i\sigma)/(V-c)$. From residue theory and the requirement that the solution, ζ_{1p}, obtained from these poles be bounded everywhere, we find

$$\zeta_{1p}(x,y,t) = \pm\zeta_p(x,y,t)H[\pm(y+ct)], \tag{6.3}$$

where
$$\zeta_p(x,y,t) = P\frac{\gamma^2}{(V-c)^2}\frac{f\omega}{\rho g}\exp\left[-\frac{f}{c}(x+x_0)\right]\exp[-|m|(y+ct)]$$
$$\times\{\cos[\kappa(y+ct)]+\alpha\sin[\kappa(y+ct)]\}, \quad (6.4)$$

$\alpha = \sigma/\omega$, $(\kappa, m) = (\omega,\sigma)/(V-c)$ and where we use $+$ for $c > V$, $-$ for $c < V$.

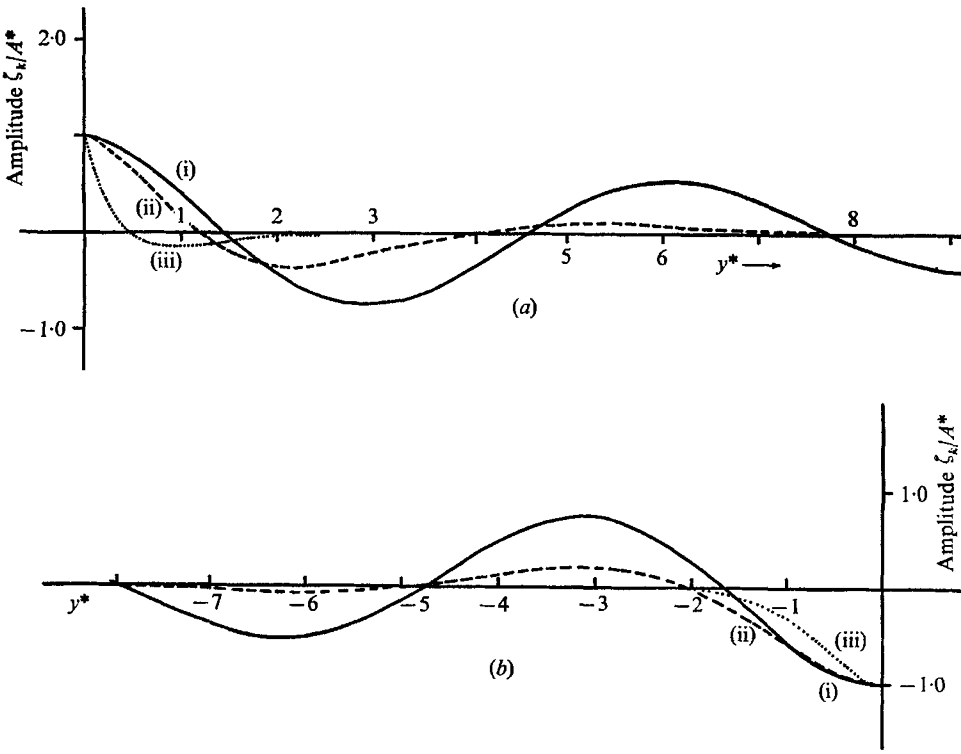

FIGURE 4. Plot of the amplitudes of the pressure-generated Kelvin waves with respect to: (a) the leading edge ($c > V$), and (b) the trailing edge ($V > c$), for various values of σ: (i) $\sigma = \frac{1}{10}\omega$; (ii) $\sigma = \frac{1}{2}\omega$; (iii) $\sigma = 2\omega$. The edge for $y = -Vt$ is not shown; fixing it on the figure determines ωt.

$$y^* = \frac{\omega}{|V-c|}(y+ct); \quad A^* = P\frac{\gamma^2 f\omega}{(V-c)^2\rho g}\exp\left(-\frac{f}{c}x_0\right).$$

As in the previous example we next evaluate the first term of (3.8) at the poles in the s plane due to the force, (6.2). These poles, at $s_{\pm} = -i(\lambda V \pm \omega)-\sigma$, contribute a response ζ_{2p}, in which

$$\zeta_{2p}(x,y,t) = \pm(-)\zeta_p(x,y,t)H[\pm(y+Vt)] \quad (6.5)$$

with $\pm$ having the same meaning as in (6.4). The Kelvin-wave response, ζ_k, formed from the sum of (6.3) and (6.5) is given by

$$\zeta_k(x,y,t) = \zeta_p(x,y,t)\{H[\pm(y+ct)]-H[\pm(y+Vt)\}\operatorname{sgn}(c-V). \quad (6.6)$$

As seen from figures 3(a) and (b), ζ_k as given by (6.6) occupies two distinct longshore regions with respect to the storm, depending on the sign of $c-V$. For $c > V$

the Kelvin waves move away from the storm region at group velocity c, and at wave-number $\kappa = \omega/(c-V)$. For $c < V$ there is a Kelvin-wave 'wake' travelling in the storm direction. If we transform $V \to -V$, to give a storm moving in the positive y direction, we find a Kelvin wave in the region $-ct < y < Vt$. Figures 4(*a*) and (*b*) are plots of these Kelvin-wave solutions for various values of σ/ω for the cases $V < c$ and $V > c$ respectively. The co-ordinates are fixed at $y = -ct$ with the edge $y = -Vt$ not shown, in order to show the full wave development. If we choose the position of this edge, then y^*, at $y = -Vt$, becomes $y^* = -\omega t$ so that t is determined for each ω. This also fixes the region occupied by the wave whose leading or trailing edge ($V > c$ or $V < c$) decays at the same rate as the amplitude of the storm.

In the present theory we interpret: (i) the delta function as the limit of a Gaussian pressure distribution, viz.

$$\delta(z) = \lim_{\epsilon \to 0^+} \frac{1}{\epsilon \pi^{\frac{1}{2}}} \exp(-z^2/\epsilon^2) \tag{6.7}$$

and (ii) $\gamma = \gamma(\epsilon)$ to be much larger than the wavelength of gravity waves but still much smaller than the characteristic horizontal wave scales $(c/f, \kappa^{-1})$. For example, if in (6.1) we had started with a Gaussian distribution in the x direction, centred about x_0, we would have obtained an x dependence for ζ_p of (6.4) as

$$\zeta_p(x) \propto \exp[-f(x+x_0)/c] \exp[(f\epsilon/c)^2] \tfrac{1}{2}[1+\operatorname{erf}(b/\epsilon)], \tag{6.8}$$

where $\operatorname{erf}(q)$ is the error function and $b = \frac{1}{2}(2x_0 - f\epsilon^2/c)$. In the limit $\epsilon \to 0^+$, $\zeta_p(x) \to \exp[-f(x+x_0)/c]$, $x_0 > 0$, as required.

The important point here, however, is that since f/c is small ($\sim 10^{-3}\,\text{km}^{-1}$) ϵ (or γ) need not be too small before (6.8) is closely approximated by the first term only, hence justifying the use of the delta function to represent a storm of finite width. To demonstrate these remarks we note that if $b/\epsilon = 2$ then the $\operatorname{erf}(2) = 0{\cdot}995\ldots$, which for $\epsilon \sim O(10^2\,\text{km})$ also implies that $\exp[(f\epsilon/c)^2] \sim 1{\cdot}22\ldots$. We note further that $b/\epsilon \sim x_0/\epsilon$ for the above value of ϵ, which in turn implies that $x_0 = 2\epsilon$ represents a storm of Gaussian thickness ϵ centred offshore at a distance of about 200 km.

Of some interest is the case $V \to c$ for a storm moving in the negative y direction. This limit must be applied with care, however, since in modelling the storm we have assumed γ^{-1} much larger than the horizontal wave-numbers (κ, m). The result of applying $V \to c$ for finite m is that there will be a large surface discontinuity at the leading (trailing) edge $y = -ct$ for $c > V(c < V)$. Immediately behind (in front), $y+ct > 0$ $(y+ct < 0)$, the surface will decay rapidly to zero. Finally, in the limit $V = c$ there will be no waves, as expected, since this also implies $\omega = 0$.

We omit any discussion of the remaining pressure terms of (3.8) except to point out that the last term corresponds to the direct surface response to the force.

Also, it should be noted that $\sin \omega t$ was used in the preceding examples to determine the effect of a time-variable force amplitude. If we consider that the atmospheric force, and resulting long-wave sea surface response, can be Fourier analyzed into a sum of sine and cosine components, we could regard the chosen forcing fields as representing one component of the Fourier expansions. In the absence of an oscillatory forcing field, the response becomes simply a moving Kelvin-type 'surge'.

7. Steady-state solutions

As a result of the awkward integrals that arise when attempting to evaluate the full surface response it is desirable to know the response in the limit $t \to +\infty$ (the steady-state solution) without having to approximate the integrals individually. To this end we use the final value theorem,

$$\lim_{t \to +\infty} \zeta(x, y, t) = \zeta(x, y) = \lim_{s \to 0^+} s\mathscr{L}[\zeta(x, y, t)] \tag{7.1}$$

(where $\mathscr{L}$ is the Laplace transform) provided $\zeta(x, y, t)$ is a piecewise continuous function for $t \geqslant 0$ and has a limit as $t \to +\infty$, s approaching 0^+ through real values. Application of the above limit to

$$\mathscr{L}[\zeta(x, y, t)] = \mathscr{F}^{-1}[\bar{\zeta}(x, \lambda, s)] \tag{7.2}$$

in which $\mathscr{F}^{-1}$ is the inverse Fourier transform, for the examples chosen in §§ 5 and 6, shows that in each case

$$\lim_{t \to +\infty} \zeta(x, y, t) = 0;$$

the surface returns to its original state of rest.

8. Physical discussion of the solutions ζ_k

In this section we will give a physical interpretation to the Kelvin-wave solutions obtained in the previous sections.

When a wind is suddenly applied to one-half of the bounded sea, there is immediate motion in the direction of the stress. The discontinuity at the boundary of the generating area will then begin to move away at group velocity $(gh)^{\frac{1}{2}}$ and to be effected by the rotational forces. Such forces will tend to turn motions to the right (left) of their direction of propagation in the northern (southern) hemisphere. The requirement of zero normal velocity at the wall, however, restricts the formation of a transverse motion outside the forcing region. As a result, for motions having the boundary to the right of their direction of propagation, a surface slope must exist to balance the Coriolis force. No Kelvin waves can exist in the generating region for the case considered; forced waves in this region, however, have their wave-numbers modified by the rotational effects [(5.6)–(5.9)]. The original y dependence of the stress is felt through the propagating surge given by the last term of (5.5).

For the case of pressure-generated Kelvin waves, we base the discussion on the result obtained in § 6 in which we considered the x dependence of the atmospheric pressure as a limit of a Gaussian distribution. Since the storm's influence would extend to the boundary, any long wave motion set up by the force will have its onshore velocity component restricted by the wall. The Coriolis force will again be balanced by a sloping sea surface as in the first example. But now, because of the smallness of the atmospheric pressure gradient at the coast for storms far offshore (i.e. large x_0) as compared to those near the coast, the slope of the sea surface need not be as large to give a balance. This is clearly manifested in (6.4) by the weighting function $\exp(-fx_0/c)$. The direct dependence of the amplitude of (6.4) on f shows that these waves are a direct result of the rotation and are not a modification of a surge as in the wind-stress example. Finally, the change of the natural frequencies of the storm (σ, ω) to $(\sigma, \omega)/(V \pm c)$ in the Kelvin waves is the common 'Doppler' effect for waves generated by a moving source.

9. Numerical values for the Oregon coast

One appropriate region for a numerical discussion of the amplitudes and velocities of the wind- and pressure-generated Kelvin waves is the Oregon coast of the United States. This straight, north–south running coast approximates the wall of the mathematical model, with the north–south wind component being dominant and the offshore movement of relatively small storms being common, especially in the winter. Also, numerous tide gauges afford the possibility of detecting these waves through the analysis of simultaneous sea level records.

An important feature of any real ocean, however, as opposed to the constant depth model, is the existence of a continental shelf and slope between the coast and the ocean basin. The added complications due to such rapid topographic change might be enough to obscure the Kelvin waves generated.

$(\sigma, \mu c)/\omega$	A (cm)
$(1, 1)$	6·0
$(1, \frac{1}{2})$, $(\frac{1}{2}, 1)$	4·7
$(2, \frac{1}{2})$, $(\frac{1}{2}, 2)$	1·8

TABLE 1. Kelvin wave amplitude A at $x = 0$. $\tau_0 = 1$ dyne/cm^2; $\rho = 1$ g/cm^3; $g = 10^3$ cm/sec^2; $h = 2000$ m; $\omega = 0{\cdot}12 \times 10^{-4}$ sec^{-1}.

In table 1 the maximum amplitudes, A, of the wind-generated Kelvin waves of § 5 are presented for the various values of $(\sigma - \mu c)/\omega$ used in the plots of figure 2; A is given by (5.4). The calculations are for $\tau_0 = 1$ dyne/cm^2 and $\omega = 0{\cdot}12(10^{-4})$ sec^{-1} (day^{-1}) only, since A is directly proportional to τ_0 and inversely proportional to $\omega(\neq 0)$. As an example of the magnitude and variability of the northward wind-stress off Oregon, data obtained by Oregon State University for the period 1 Aug. to 31 Sept. 1966 are presented in figure 5 (Mooers *et al.* 1968). These data seem to indicate the presence of a dominant period in the longshore wind-stress component during the time of observation, thus partly justifying the use of the model chosen in (5.1). Also, the period appears to be roughly 2π days, corresponding to the value of ω used above. The familiar experimental law $\tau = c'\rho_a U^2$, where $c' = 2{\cdot}5(10^{-3})$ is the drag coefficient and $\rho_a = 1{\cdot}27(10^{-3})$ g/cm^3 is the density of air, has been used to obtain the stress from the mean wind speed U.

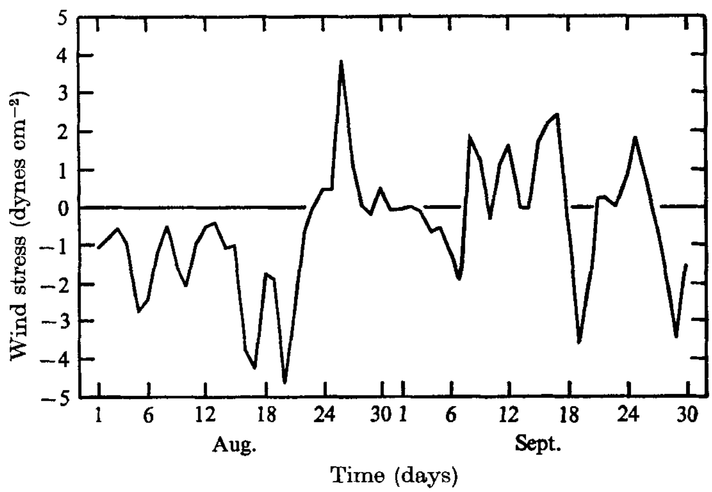

FIGURE 5. Daily northward wind-stress off the Oregon coast from 1 Aug. to 31 Sept. 1966.

The maximum coastal amplitude, A^*, of the pressure generated Kelvin waves of §6 are given in table 2; $A^* = P[\gamma^2 f\omega/(V-c)^2\rho g]\exp(-fx_0/c)$. We consider $V \ll c$ only, since for typical storms V is usually less than 40 km/h, while for an ocean depth of 2000 m, $c = (gh)^{\frac{1}{2}} = 504$ km/h. Also, we will take

γ (km)	V (km/h)	x_0 (km)	A^* (cm)
100	40	100	$0{\cdot}4(10^{-1})$
200	100	100	$0{\cdot}2$
100	40	1000	$0{\cdot}1(10^{-1})$
1000	40	1000	$2{\cdot}0$

TABLE 2. Kelvin wave amplitudes A^* at $x = 0$. $P = 50\times10^3$ dynes/cm^2; $f = 1{\cdot}03\times10^{-4}$ sec^{-1}; $\rho = 1$ g/cm^3; $h = 2000$ m; $\omega = 0{\cdot}12\times10^{-4}$ sec^{-1}.

$P = 50$ mb $= 50(10^3)$ dynes/cm^2 as representative of an intense storm having a Gaussian thickness γ. As for table 1 only $\omega = 0{\cdot}12(10^{-4})$ sec^{-1} will be considered since A^* is directy proportional to ω. As might be expected, the amplitudes of the pressure-generated waves are much less than those generated by the wind.

I would like to thank Dr L. A. Mysak for his assistance in the early stages of this work, Mr M. Manton for helpful discussions and the referee for pointing out a basic error in the original paper.

Also, I am grateful to the National Research Council of Canada for their financial support.

REFERENCES

CARRIER, G. F., KROOK, M. & PEARSON, C. E. 1966 *Functions of a Complex Variable.* New York: McGraw-Hill.

CREASE, J. 1956 Propagation of long waves due to atmospheric disturbances on a rotating sea. *Proc. Roy. Soc.* A **223**, 556–569.

KAJIURA, K. 1962 A note on the generation of boundary waves of the Kelvin type. *J. Oceanographic Soc. Japan*, **18** (2), 51–58.

LONGUET-HIGGINS, M. S. 1965 The response of a stratified ocean to stationary or moving wind systems. *Deep-Sea Res.* **12**, 923–973.

MOOERS, C. N. K., BOGERT, R. L., SMITH, R. L. & PATTULLO, J. G. 1968 A compilation of observations from moored current meters and thermographs (and of complementary oceanographic and atmospheric data). *Department of Oceanography, Oregon State University*, vol. 2.

MYSAK, L. A. 1969 On the generation of double Kelvin waves. *J. Fluid Mech.* **37**, 417–434.

VERONIS, G. & STOMMEL, H. 1956 The action of variable wind stresses on a stratified ocean. *J. Marine Res.* **15**, 45–75.